

BLR Modeling: A New Approach

Shai Kaspi and Hagai Netzer

School of Physics and Astronomy and the Wise Observatory, The Raymond and Beverly Sackler Faculty of Exact Sciences, Tel-Aviv University, Tel-Aviv 69978, Israel

Abstract.

We present a new scheme for modeling the broad line region in active galactic nuclei. It involves photoionization calculations applied to a number of variable emission lines at *all times*. We demonstrate how fitting all lines simultaneously provide strong constraints on several of the more important parameters, such as the density and column density, and the radial distribution of the emission line clouds.

When applying the model to the Seyfert 1 galaxy NGC 5548, we are able to reconstruct the light curves of four emission-lines, in time and in absolute flux. We argue that the Balmer line light curves, and possibly also the Mg II $\lambda 2798\text{\AA}$ light curve, do not fit this scheme because of the limitations of present-day photoionization codes. We rule out models where the particle density scales as r^{-2} and favor models where it scales as $r^{-(1-1.5)}$. We can place lower limits on the column density at a distance of 10 ld, of $N_{col}(r=10) \gtrsim 10^{22} \text{ cm}^{-2}$, and limit the particle density to be in the range of $10^{11} > N(r=10) > 10^{9.5} \text{ cm}^{-3}$.

1. Introduction

Broad emission line regions (BLRs) in Active Galactic Nuclei (AGNs) have been the subject of extensive studies for more than two decades. Such regions are not spatially resolved, and all the available information about their geometry is obtained from analysis of variable lines. It is well established that photoionization by the central radiation source is the main source of ionization and excitation of the BLR gas. Indeed, photoionization calculations, when applied to time-averaged spectra, can reasonably explain most of the observed line ratios (for review and references see Ferland, in these proceedings, and Netzer 1990). However, such time-averaged calculations contain little information about the spatial distribution of the gas.

Extensive monitoring campaigns, during the last decade, have produced several high quality data sets. They include the time dependence of the multi-wavelength continuum, as well as the change in line fluxes and line profiles as a function of time (for a review see, Horne — these proceedings, Peterson 1993, Netzer & Peterson 1997). Excellent data sets are now available for half a dozen low luminosity AGNs. Less complete (in terms of wavelength coverage) yet very detailed data sets, are available on a dozen or so more sources.

Unfortunately, theoretical understanding lags behind and there are few, if any, systematic attempts to produce complete BLR models that reproduce the new light curves. Most recent studies focused on obtaining transfer functions, and little effort has been devoted to reconstruct the physical conditions in the gas. In particular, only one or two emission lines have been considered while many more lines, and thus more information and constraints, are available, at least in some data sets.

This work, as well as the more detailed results in Kaspi and Netzer (1999), present an attempt to investigate one of the best data sets in a new way. The goal is to reconstruct the observed light curves of as many emission lines as possible in the Seyfert 1 galaxy NGC 5548. As shown below, the observational constraints on the line intensity and line ratios as a function of time, enable us to deduce the run of density, column density and cloud distribution across the BLR in this source. Below we demonstrate how the time dependent relative and absolute line intensities, and their relationship to the variable continuum, leave little freedom in modeling the BLR.

2. Previous models

Previous attempts to model the BLR differ in the method used to reconstruct the gas distribution and the assumptions made about the BLR properties. We distinguish between direct and indirect methods. Direct methods involve initial guess of the gas distribution and other properties. These are later checked by calculating the predicted emission line light curves, assuming the above properties and the given variable continuum. Indirect methods attempt to obtain the gas distribution by computing transfer functions for various emission lines. This is somewhat ill-defined since it produces emissivity maps, rather than mass-distribution maps. It therefore requires an additional confirmation that the so-obtained emissivity maps are consistent with photoionization calculations. While there were several attempts to produce transfer functions for various lines, we are not aware of any successful mapping that is consistent with full photoionization calculations (see also Maoz 1994).

The first systematic attempt to reconstruct the BLR in NGC 5548 is by Krolik et al. (1991). These authors used the Maximum Entropy Method to reconstruct the transfer function and to model the BLR as a spherically symmetric system of isotropically emitting clouds. The Krolik et al. BLR is divided into two distinct zones: one emitting the high-ionization lines (column density of $\sim 10^{22}$ cm $^{-2}$ and ionization parameter of 0.3) and the other emitting the low-ionization lines (column density of $\sim 10^{23}$ cm $^{-2}$ and ionization parameter of 0.1). Later, O'Brien, Goad, & Gondhalekar (1994) have combined photoionization and reverberation calculations (§ 3.). Their study, and also the one by Pérez, Robinson & de la Funte (1992), focused on the shape of the transfer function under different conditions and on the line emissivity for a few generic models. They did not attempt any detailed reconstruction of a specific data set.

Bottorff et al. (1997) presented a detailed kinematic model, combined with photoionization calculations. This was applied to only *one line* (C IV $\lambda 1549\text{\AA}$) in the spectrum of NGC 5548. Dumont, Collin-Suffrin, & Nazarova, (1998) modeled the BLR in NGC 5548 as a 3 zones region where the various com-

ponent locations are determined by *average* line-to-continuum lags. Much of their conclusions regarding the required density and column density are based on the relative strength of the Balmer lines. Finally, Goad & Koratkar (1998) re-examined the same NGC 5548 data set and deduced a strong radial dependence ($N \propto r^{-2}$ over the density range of $10^{11.3} - 10^{10.0} \text{ cm}^{-3}$). Here again, the main assumption is of a simple two zone model and the photoionization calculations are not applied to all the lines. None of the above models presents a complete study or attempts full recovery of all light curves. Hence, global consistency checks are missing.

Our work relies heavily on the direct approach. We prefer to avoid, as much as possible, ill-defined transfer functions and unreliable emissivity distributions. Instead, we make a large number of initial assumptions (“guesses”) and check them, one by one, against the complete data set. This makes the numerical procedure more time-consuming but is more robust because of the direct relationship between the assumed geometry and the resulting light-curves.

3. Formalism

We follow the formalism presented in Kaspi & Netzer (1999) which is first described in Netzer (1990). The reader is referred to those references for more information. In summary, we consider a spherical BLR consisting of numerous small spherical clouds and a point-like ionizing source. All important physical properties are represented by simple power-laws in r , the distance from the central source. A possible justification for this may be a radial dependent external pressure that determines the cloud properties. The case presented here assumes isotropically emitting clouds. We are fully aware of the potential complications due to this assumption, in particular for lines like $L_{y\alpha}$.

The particle density in the model, $N(r)$ (assumed to be constant within each cloud), is given by

$$N(r) \propto r^{-s} \quad . \quad (1)$$

The cloud column density, N_{col} , is computed by considering spherical clouds, of radius $R_c(r)$. The mass of the individual clouds is conserved, but it is not necessarily the same for all clouds, thus, $R_c^3(r)N(r) = const$. The typical cloud column density is

$$N_{col}(r) \propto R_c(r)N(r) \propto r^{-2/3s} \quad , \quad (2)$$

and the geometrical cross-section is

$$A_c(r) \propto R_c^2(r) \propto r^{2/3s} \quad . \quad (3)$$

The number density of such clouds per unit volume is

$$n_c(r) \propto r^{-p} \quad . \quad (4)$$

The clouds are illuminated by a central source whose ionizing luminosity, $L(t)$, varies in time. Designating $\epsilon_l(r, L)$ as the flux emitted by the cloud in a certain emission-line – l per unit projected surface area ($\text{erg s}^{-1} \text{ cm}^{-2}$), we find the following relation for a single cloud emission:

$$j_{c,l}(r) = A_c(r)\epsilon_l(r, L) \quad . \quad (5)$$

Assuming the system of clouds extends from r_{in} to r_{out} we integrate over r to obtain cumulative line fluxes:

$$E_l \propto \int_{r_{in}}^{r_{out}} n_c(r) j_{c,l}(r) r^2 dr \quad . \quad (6)$$

Having determined the properties of the emission line clouds, and having assumed a spectral energy distribution (SED) for the ionizing source, we now calculate $\epsilon_l(r, L)$ using a photoionization code and follow the formalism to obtain E_l .

We also consider the changes of L , and possibly also the SED, in time. We take this into account by calculating $\epsilon_l(r, L(t))$ for the entire range of continuum luminosity applicable to the source under discussion. The calculated line fluxes are the results of integrating Eq. 6, using, at each radius, the relevant ionizing flux, i.e. the one obtained with the ionizing luminosity $L(t - r/c)$.

A model is specified by the source luminosity and SED, the radial parameter s , and the normalization of the various free parameters. These include p , r_{in} , r_{out} and the density and column density at a fiducial distance which we take to be one light-day. The comparison with observations further requires the normalization of the total line fluxes and hence the integrated number of clouds (an alternative way of presenting this normalization is by defining a radial dependent covering fraction).

We have calculated a large grids of photoionization models covering the entire range of density, column density, and incident flux applicable for this source. The calculations were performed using ION97, the 1997 version of the code *ION* (see Netzer 1996, and references therein). There are several limitations for such codes which should be considered. Most important (and crucial for any BLR model) is the transfer of the optically thick lines. This is treated with a simple, local escape probability method which has long been suspected to be inadequate for the Balmer lines (see Netzer 1990). The problem is not yet solved and is common to most detailed photoionization models similar to *ION*, like *Cloudy* by G. Ferland. There is no simple solution for this problem and we prefer, at this stage, not to consider Blamer lines in this work. There is a similar problem for several other low ionization lines, like Mg II $\lambda 2798\text{\AA}$ and the Fe II lines. On the other hand, the transfer of lines like Ly α and C IV $\lambda 1549\text{\AA}$ is much better understood.

4. A model for NGC 5548

The Seyfert 1 galaxy NGC 5548 is one of the best studied AGN. It was monitored, for 8 months, in the optical-UV, in 1989, and was also the subject of an intensive optical spectroscopic monitoring for 8 years (Peterson et al, 1999). Several shorter monitoring campaigns, each with a duration of several months, took place in various wavelength bands. This makes NGC 5548 an excellent choice for testing our model. In this study we have concentrated on the *International Ultraviolet Explorer (IUE)* 1989 campaign (Clavel et al. 1991) and used the resulting light curves of the UV continuum (at $\lambda 1337\text{\AA}$) and the following emission lines: Ly α $\lambda 1216\text{\AA}$, C IV $\lambda 1549\text{\AA}$, C III] $\lambda 1909\text{\AA}$, He II $\lambda 1640\text{\AA}$,

and $\text{Mg II } \lambda 2798 \text{ \AA}$. (All diagrams in this paper show light curves of only the first three lines.)

Several additional observational constraints have been considered:

1. The *IUE* spectra clearly show that the $\text{C III } \lambda 1909 \text{ \AA}$ line is blended with $\text{Si I } \lambda 1895 \text{ \AA}$. Clavel et al. (1991) have measured the combined flux of both lines, and listed it as $\text{C III } \lambda 1909 \text{ \AA}$. Hence, our calculated flux for both lines will be combined (see Kaspi and Netzer 1999 for more details regarding the use of this ratio as a density diagnostics).
2. The observed SED of NGC 5548 is reviewed by Dumont et al. (1998). We found a strong dependence of our results on the ratio of the UV to X-ray continuum flux. We have chosen a typical Seyfert 1 SED with $\alpha_{ox} = 1.06$ similar to the one measured for NGC 5548.
3. Using the observed $\lambda 1337 \text{ \AA}$ continuum flux, an assumed cosmology ($H_0 = 75 \text{ km s}^{-1} \text{ Mpc}^{-1}$ and $q_0 = 0.5$), and assumed SED, we have estimated a time averaged ionizing luminosity of $10^{44} \text{ erg s}^{-1}$. During the *IUE* campaign, the UV continuum flux varied by a factor of ~ 4.5 , hence we choose our grid to cover the ionizing luminosity range of $10^{43.6}$ to $10^{44.3} \text{ erg s}^{-1}$.
4. Based on reverberation mapping results, we have defined our grid of distances to cover the range of 1 to 100 light days.

Model calculations proceed in two stages. First we produce a two dimensional grid of $\epsilon_l(r, L(t))$ for several values of the parameter s . We have considered $s=1, 1.5$, and 2 , with the additional normalizations of the density at 10 light day ($N(r=10)$) in the range $10^{9.5}$ to $10^{11.5} \text{ cm}^{-3}$, and column densities ($N_{col}(r=10)$) of 10^{21} to 10^{23} cm^{-2} . In the second stage we calculate theoretical light curves by integrating over Eq. 6 with the given s , the chosen r_{in} and r_{out} , and several values of the parameter p . We have examined models with $p=1, 1.5$, and 2 for each grid. In each model we vary both r_{in} and r_{out} to minimize χ^2 . This score is calculated by comparing the theoretical and observed lines fluxes for *all chosen lines*. The smallest χ^2 determines our best parameters.

4.1. Detailed examples

To illustrate our model, we present the results of two sets of calculations. First we consider a model with $s=2$ and $p=1.5$ (This particular choice results in $N_{col}(r) \propto r^{-4/3}$). We chose $N_{col}(r=10) = 10^{22.67} \text{ cm}^{-2}$ and study the full density range. We note again that is referred to here as *a single model* covers in fact a large range of density and column density. For example, choosing $N(r=10) = 10^{10.5} \text{ cm}^{-3}$ means a full density range of $10^{9-12} \text{ cm}^{-3}$ and a full column density range of $10^{21.33-24} \text{ cm}^{-2}$.

Examining this case we note some obvious features. First, for $N(r=10) \lesssim 10^{10.2} \text{ cm}^{-3}$ the response of the modeled emission lines is reversed, i.e., increasing continuum flux results in decreasing line flux. This is demonstrated in Fig. 1 (check the dotted line in the diagram). This is a clear sign of optically thin material in the inner BLR. It is caused by a combination of large incident fluxes

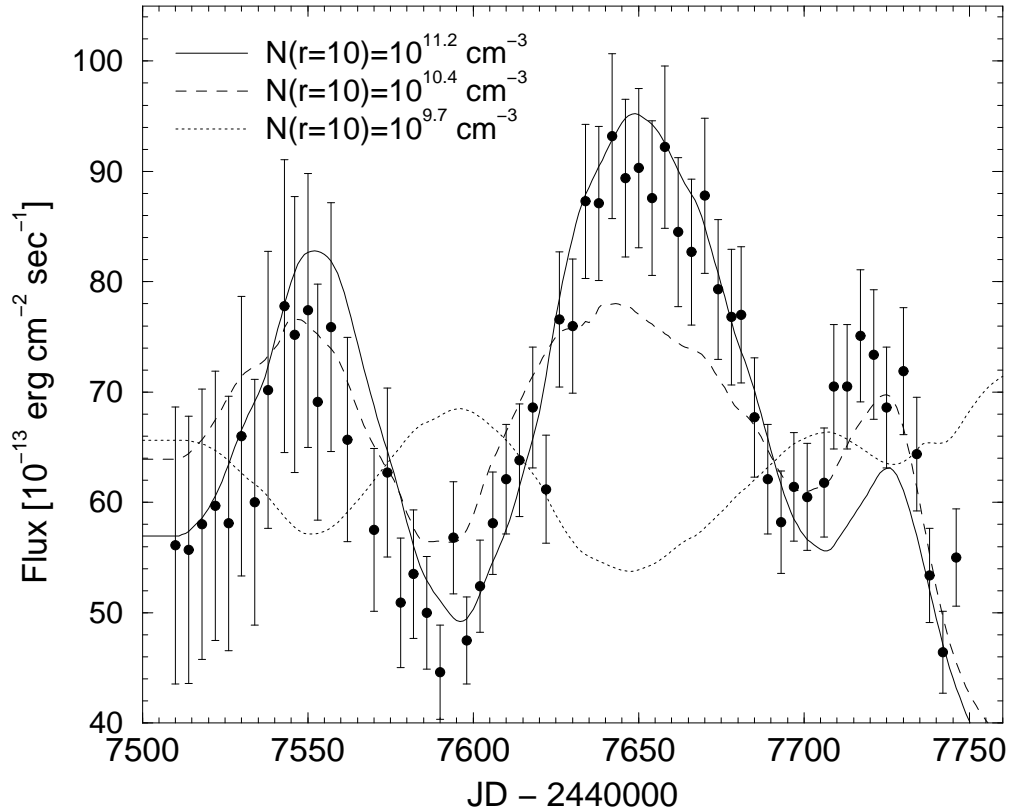


Figure 1. Ly α light curves resulted from a model with $s = 2$, $r_{in}=3$ ld, $r_{out}=25$ ld $N_{col}(r=10)=10^{22.67}$ cm $^{-2}$, and various values of $N(r=10)$ as marked. The observed light curves are from Clavel et al. (1991).

and small densities (i.e. large ionization parameters) with relatively small column density. Such models are in poor agreement with observations and smaller ionization parameters and/or larger columns must be considered.

The problem can be cured by raising the density to $N(r=10) \gtrsim 10^{10.2}$ cm $^{-3}$. The resulting light curves is in much better agreement with the observations (Fig. 1: dashed and solid lines). The reversed response in Ly α has disappeared and the theoretical line light curves nicely fit the observed ones with $r_{in}=3$ ld and $r_{out}=25$ ld assuming $N(r=10)=10^{10.4}$ cm $^{-3}$. However, applying this geometry to the other emission lines, we get unsatisfactory results. This is illustrated in Fig. 2A (solid lines) that show the improved fit to the Ly α , and C IV data and the very poor agreement for C III].

The above example demonstrate the difficulty in fitting, simultaneously, line responses and line ratios. The example illustrates why a particular radial dependence, like the one used here ($s = 2$), cannot adequately fit the observed variable emission line spectrum of NGC 5548. Our simulations show that no normalization or a choice of p can cure this problem.

In the second example $s=1$ with the following normalization: $N(r=10)=10^{10.4}$ cm $^{-3}$, $N_{col}(r=10)=10^{23.33}$ cm $^{-2}$, $r_{in}=3$ ld and $r_{out}=100$ ld. The light curves are presented in Fig. 2B. This set of models give much better fit to

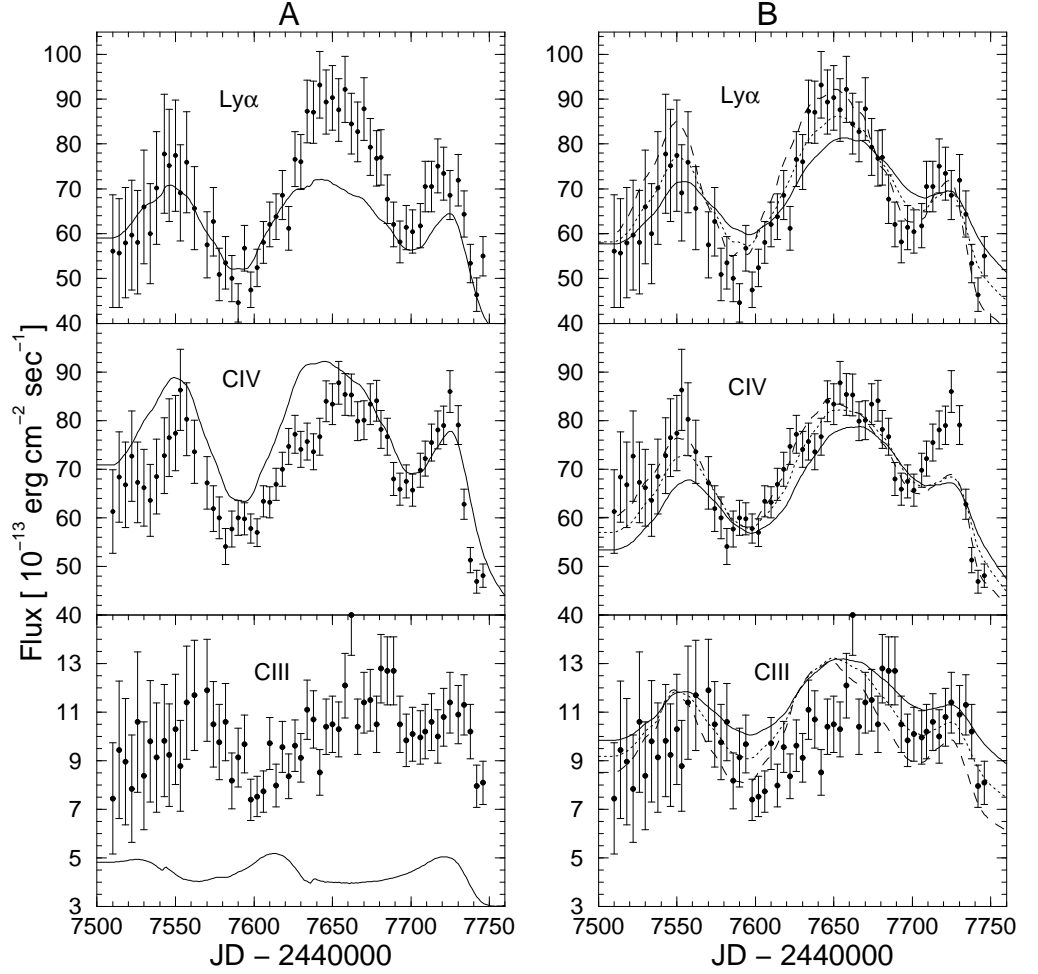


Figure 2. Simulated light-curves compared with observations:

A. A model with $s=2$, $p=1.5$, $N(r=10)=10^{10.4} \text{ cm}^{-3}$, $N_{col}(r=10)=10^{22.67} \text{ cm}^{-2}$, $r_{in}=3 \text{ ld}$, and $r_{out}=25 \text{ ld}$. The bad disagreement between the observed and theoretical light curve is typical to all $s = 2$ models.

B. A model with $s=1$, $N(r=10)=10^{10.4} \text{ cm}^{-3}$, $N_{col}(r=10)=10^{23.33} \text{ cm}^{-2}$, $r_{in}=3 \text{ ld}$, and $r_{out}=100 \text{ ld}$. Models for different values of p are presented: solid line - $p=1$; dotted line - $p=1.5$; dashed line - $p=2$.

the data (note in particular the C III] light-curve). Comparing both models demonstrate the usefulness of this approach in constraining the parameter space.

4.2. General trends

We have checked a large range of model parameters and comment, below, on several of the more obvious trends.

We first note that as the column density grows from $N_{col}(r=10)=10^{21}$ to 10^{23} cm^{-2} , the agreement with the observations is much better. Thus, models with $N_{col}(r=10)=10^{21} \text{ cm}^{-2}$ do not fit the observations while $N_{col}(r=10)\gtrsim 10^{22} \text{ cm}^{-2}$ already results in a reasonable agreement. Photoionization codes like the one used here, are limited to column density less than about 10^{25} cm^{-2} (i.e. Compton thin clouds). Hence we are unable to put an upper limit on the column density.

Using models with $s=1.5$ and $s=1$, we can obtain lower and upper limits on the gas density. Models with $N(r=10)\lesssim 10^{9.5} \text{ cm}^{-3}$ do not fit the observation (in the $s=1.5$ models there is a reverse response of the lines and in the $s=1$ models the line ratios do not agree with the observations). For $N(r=10)\gtrsim 10^{11} \text{ cm}^{-3}$, the line ratios for both value of s do not agree with the observations. Hence we find the BLR density of NGC 5548, in our model, to be in the range of $10^{11} > N(r=10) > 10^{9.5} \text{ cm}^{-3}$.

A general trend for all values of s is that as p increases from 1 to 2 (i.e., more weight is given to clouds closer to the central source) the amplitude of the modeled light curves is in better agreement with the observations and so are most line ratios. Hence, models with higher p are preferred.

A common problem for all models is the weak Mg II $\lambda 2798\text{\AA}$ line. While we do not have a complete explanation for this, we suspect it is due to one of two reasons: either the transfer of this line is inaccurate, similar to the case of the Balmer lines, or else it is caused by the thousands of highly broadened Fe II lines, in that part of the spectrum, that make the measured line intensity highly uncertain (see for example the discussion in Wills, Wills and Netzer, 1985; Maoz et al. 1993) (a third possibility of enhanced metallicity is discussed in Kaspi and Netzer 1999). Our χ^2 evaluation does not include the Mg II line. This is a definite failure of the model.

Another common trend is the improvement of the χ^2 score with increasing r_{out} . This is most noticeable as r_{out} increases from 50 to 100 light days.

Considering all the above trends and limitations, and using the χ^2 score, we find that models with $s=1$ best fit the observed spectra and models with $s=1.5$ give somewhat inferior fits. An example of one of our best models is shown in Fig. 2B. In this model the reduced χ^2 score for the four lines is 4.5 for the $p=1$ model, 3.1 for the $p=1.5$ model, and 2.2 for the $p=2$ model. The total covering factors found for these models are 0.25, 0.28. and 0.30, respectively.

5. Discussion

Our direct method allow us to investigate, in a critical way, a large variety of BLR models. Unlike indirect methods that are based on transfer function of individual lines, and make no use of their relative or absolute intensity, we are able to introduce many more observational constraints. The χ^2 minimization

applied to 4 emission lines, at *all times*, enable us to choose among various models and to rule out cases of unsuitable density, column density and covering fraction. In particular we were able to show that:

1. There is a narrow range of density and density dependence that fit the observed light curves. Using our parameters we find that s is in the range of 1–1.5 and the largest density (at one light day) is about $10^{12.5} \text{ cm}^{-3}$. The simulations rule out steep density laws like $s = 2$. This is in disagreement with the results of Goad & Koratkar (1998) despite of the fact that their range of acceptable densities ($N \sim 10^{11.3} \text{ cm}^{-3}$ in the inner BLR and $N \sim 10^{10.0} \text{ cm}^{-3}$ in the outer BLR) is similar to ours and their deduced lower limit on the column density is also in agreement with ours. We suspect that Goad & Koratkar’s conclusion about the good fit of the $s = 2$ case is related to their use of mean time lags rather than compared with our detailed fit to the light curves.
2. Detailed emission line variability can be used to put useful constraints on the column density of clouds across the BLR. Realistic models require large enough columns to avoid optically thin clouds at small distances.
3. Simple two or three zone models contain too little information and hence cannot constrain, accurately enough, the physical conditions in the gas. For example Dumont et al. (1998) have used a three zone model and reached several conclusions based on time-averaged properties. They noted three problems arising from their modeling: an energy budget problem, a line ratio problem, and a line variation problem. The first two are most probably related to the Balmer line intensity and, as explained, we suspect this to be a general limitation of current photoionization models. Regarding the line intensity, we find good agreement for both high and low ionization lines and suspect that even a three-zone model is highly simplified for the purpose of realistic reconstruction of the BLR.
4. Several recent ideas about the BLR can be tested against real observations by using an approach similar to ours. ‘Locally Optimally-emitting Clouds’ (LOCs) models (Baldwin et al. 1995, Korista et al. 1997) have been suggested to explain the broad line spectrum of AGNs. The models assume that there are clouds with a range of density and column density at each distance. LOCs must be put into a real test by checking whether they result in light curves that are in better agreement with the observations, compared with the simpler models assumed here.

Alexander & Netzer (1997) have suggested that the BLR clouds may be bloated stars (BSs) with extended envelopes. In their work they fitted the emission-line intensities, profiles and variability to mean observed properties of AGNs. One of the conclusion is that the density at the external edge of the BSs (the part emitting the lines) falls off like $r^{-1.5}$, and the number density of BSs falls off like r^{-2} . These two trends are in good agreement with our preferred values of s and p . While the model is consistent with mean time-lags of intermediate luminosity AGNs, it remains to be seen whether it can fit, in detail, the time dependent spectrum of objects like NGC 5548.

There are obvious limitations and several ways to improve our models. First, different abundances ought to be considered. Second, line beaming (anisotropy in the emission line radiation pattern) must be considered. Unfortunately, similar to the Balmer line problem, the radiation pattern cannot be accurately calculated in present-day escape-probability based codes. Multi-component models, with a range of density and column density at each radius (not necessarily similar to the LOC distribution), must be tested too. Finally, a variable shape SED (Romano and Peterson 1998) is a likely possibility that may affect the outcome of such models. Some of these additional factors are addressed in Kaspi and Netzer (1999). Others must await future work.

Acknowledgments. This work is supported by a special grant from the Israel Science Foundation.

References

- Alexander, T., & Netzer, H. 1997, MNRAS, 284, 967
- Baldwin, J., Ferland, G., Korista, K., & Verner, D. 1995, ApJL, 455, L119
- Bottorff, M., Korista, K.T., Shlosman, I., & Blandford, D.R. 1997, ApJ, 479, 200
- Clavel, J., et al. 1991, ApJ, 366, 64
- Dumont, A.-M., Collin-Suffrin, S., & Nazarova, L. 1998, A&A, 331, 11
- Goad, M., & Koratkar, A. 1998, ApJ, 495, 718
- Kaspi, S., & Netzer, H. 1999, in preparation
- Korista, K., Baldwin, J., Ferland, G., & Verner, D. 1997, ApJS, 108, 401
- Krolik, J.H., Horne, K., Kallman, T.R., Malkan, M.A., Edelson, R.A., & Kriss, G.A. 1991, ApJ, 371, 541
- Maoz, D. 1994, in Reverberation Mapping of the Broad-Line Region in AGN, eds. P.M. Gondhalekar, K. Horne, & B.M. Peterson (San Francisco: ASP), 95
- Maoz, D. et al. 1993, ApJ, 404, 576
- Netzer, H. 1990, in *Active Galactic Nuclei* eds., T.J.-L. Courvoisier and M. Mayor (Berlin: Springer-Verlag)
- Netzer, H. 1996, ApJ, 473, 781
- Netzer, H., & Peterson, B. M. 1997, in *Astronomical Time Series* eds., D. Maoz, A. Sternberg, and E. Leibowitz (Dordrecht: Kluwer Academic Publishers)
- O'Brien, P.T., Goad, M.R., & Gondhalekar, P.M. 1994, MNRAS, 268, 845
- Pérez, E., Robinson, A., & de la Fuente, L. 1992, MNRAS, 256, 103
- Peterson, B.M. 1993, PASP, 105, 247
- Peterson, B.M., et al. 1999, ApJ (in press).
- Romano, P., & Peterson, B.M. 1998, in *Structure and Kinematics of Quasars Broad Line Regions*, eds. Gaskell, C.M., Brandt, W.N., Dietrich, M., Dultzin-Hacyan, D., and Eracleous, M. (San Francisco: ASP)
- Wills, B.J., Wills, D., and Netzer, H. 1985, ApJ, 288, 94